Stellar modeling central parts of a Sun-like star.

Candidate number 24
(Dated: July 13, 2023)

The energy produced in the core is transported throughout the star either by radiation or convection. This project aims to create a Sun-like model including both mechanisms. The final model should have luminosity, mass, and radius going to 0 (or at least within 5% of initial conditions), a core reaching out to at least $0.1R_0$, and a continuous convection zone near the surface with a width of at least $0.15R_0$. This is achieved with initial parameters set to $0.9R_\odot$, $1.2L_\odot$, $29\bar{\rho}_\odot$, $0.5T_\odot$, and $M_\odot$. The result is a star where mass goes to 0, luminosity to $0.041L_0$ and radius to $0.043R_0$. The core reaches out to $0.269R_0$ and the convection zone near the surface has a width of $0.162R_0$.

I. INTRODUCTION

The interior of the Sun has a temperature of 15 million degrees Kelvin! [1] This is controlled by the efficiency of the energy transport throughout the star. The energy produced in the center is transported in two ways. The first mechanism is by radiative transport which scatters photons, and the second is by large-scale gas motion called convective transport. Which of these two mechanisms dominates is dependent on the local temperature, pressure, and chemical composition.

The purpose of this project is to model the central parts of a Sun-like star including both radiative and convective energy transport. The model should fulfill the following goals:

- Has luminosity (L), mass (m), and radius (r) all going to 0 or at least within 5% of given initial conditions for L (L_0), m (M_0), and r (R_0).
- Has a core ($L < 0.995$) reaching out to at least 10% of R_0.
- Has a continuous convection zone near the surface of the star. The width of this convection zone should be at least 15% of R_0. A small radiation zone at the edge and/or a second convection zone closer to the center is acceptable, but the convective flux should be small compared to the "main" convection zone near the surface.

II. THEORY

In this model, we have the following assumptions:

- Mass fraction of each atomic species is independent of radius and given in table II.
- All elements are fully ionized.
- Produced ${}^2_1\mathrm{D}$ is immediately consumed by the next step to produce ${}^3_2\mathrm{He}$.
- We do not consider changes over time, as we are looking at a snapshot of a star at a particular moment in time.
- Ideal gas
- No heat conduction in the star, only radiation and convection.
- $\alpha_{lm} = 1$ in eq. 15.

The initial conditions for the model can be found in table I.

Table I: Initial conditions for our stellar model. Solar parameters are found in Appendix B of ref. [1]. $\bar{\rho}_\odot = 1.408 \cdot 10^3$ kg m^{-3} is the average density of the Sun.

Symbol	Name	Value
L_0	Luminosity	$1.0 \cdot L_\odot$
R_0	Radius	$1.0 \cdot R_\odot$
M_0	Mass	$1.0 \cdot M_\odot$
ρ_0	Density	$1.42 \cdot 10^{-7} \cdot \bar{\rho}_\odot$
T_0	Temperature	5770 K

The governing equations for solving the internal structure of the radiative zone of the Sun are as follows

$$\frac{\partial r}{\partial m} = \frac{1}{4\pi r^2 \rho} \tag{1}$$

$$\frac{\partial P}{\partial m} = -\frac{Gm}{4\pi r^2} \tag{2}$$

$$\frac{\partial L}{\partial m} = \varepsilon \tag{3}$$

$$\frac{\partial T}{\partial m} = \nabla \frac{T}{P} \frac{\partial P}{\partial m} \tag{4}$$

where ρ is density, r is the stellar radius, G is the gravitational constant, T is temperature and ε is the full energy generation per unit mass in a star. m is the independent variable and makes the set of equations more stable than if r was used.

In the case of radiative transport only, the expression for eq. 4 can be reduced to

$$\frac{\partial T}{\partial m} = -\frac{-3\kappa L}{256\pi^2\sigma r^4 T^3} \tag{5}$$

where κ is opacity given in units $\mathrm{m^2 kg^{-1}}$, L is luminosity of a star and σ is Stefan-Boltzmann's constant. We determine what expression for $\partial T/\partial m$ is used through the instability criterion. Before the criterion is defined, there are several quantities that need to be defined first.

A. Flux

As we only consider radiation and convection, the total flux is given by

$$F_{\mathrm{rad}} + F_{\mathrm{con}} = \frac{16\sigma T^4}{3\kappa\rho H_P}\nabla_{\mathrm{stable}} \tag{6}$$

where ∇_{stable} is the temperature gradient needed for all the energy to be carried by radiation [1], and H_P is the pressure scale height (derived in appendix A 1)

$$H_P = \frac{k_B T}{\mu m_u g} \tag{7}$$

k_B is the Boltzmann constant, m_u is the atomic mass unit, μ is the mean molecular weight, and g is the gravitational acceleration that varies with mass. The radiative flux is

$$F_{\mathrm{rad}} = \frac{16\sigma T^4}{3\kappa\rho H_P}\nabla^* \tag{8}$$

where ∇^* is the actual temperature gradient. The convective flux can be found by taking the total flux and subtracting the radiative flux. Generally, the total energy flux at any point in the star has to obey

$$F_{\mathrm{rad}} + F_{\mathrm{con}} = \frac{L}{3\kappa\rho H_P} \tag{9}$$

B. Temperature gradients

There are four different types of temperature gradients that need to be considered: $\nabla_{\mathrm{stable}}, \nabla^*, \nabla_{\mathrm{p}}$, and ∇_{ad}. ∇_{stable} is found by equating eq. 6 and eq. 9 which yields

$$\nabla_{\mathrm{stable}} = \frac{3L\kappa\rho H_P}{64\pi r^2\sigma T^4} \tag{10}$$

The adiabatic temperature gradient ∇_{ad} is the case where the parcel temperature, density, and pressure are the exact same as the surroundings after the parcel has moved. This quantity is defined as

$$\nabla_{\mathrm{ad}} = \frac{P\delta}{T\rho c_P} = \frac{2}{5} \tag{11}$$

for an ideal gas, δ simplifies to 1, and the adiabatic temperature gradient simplifies to 2/5. The specific heat capacity, c_P is given by

$$c_P = \frac{5}{2}\frac{k_B}{\mu m_u} \tag{12}$$

The expression for the actual temperature gradient, i.e. the temperature gradient of the star, ∇^* is derived in section A 5

$$\nabla^* = \xi^3 + Uk\xi + \nabla_{\mathrm{ad}} \tag{13}$$

where k is given by

$$k = U\frac{S}{Qdl_m} = \underbrace{\frac{64\sigma T^3}{3\kappa\rho^2 c_P}\sqrt{\frac{H_P}{g\delta}}}_{U}\cdot\underbrace{\frac{4}{l_m}}_{S/Qd}\cdot\frac{1}{l_m} \tag{14}$$

the quantities U and S/Qd can be found derived in appendix A 2 and A 3. l_m is the mixing length defined as

$$l_m = \alpha_{l_m} H_P \tag{15}$$

The quantity ξ is found by solving the following cubic polynomial derived in appendix A 5

$$\xi^3 + l_m^{-2}U\xi^2 + l_m^{-2}Uk\xi - l_m^{-2}U(\nabla_{\mathrm{stable}} - \nabla_{\mathrm{ad}}) = 0 \tag{16}$$

The solution to ξ is the real root.
The temperature gradient of the parcel is found by rearranging eq. A14

$$\begin{aligned}(\nabla_p - \nabla_{\mathrm{ad}}) &= \frac{32\sigma T^3}{3\kappa\rho^2 c_p v}\frac{S}{Qd}(\nabla^* - \nabla_p)\\ \Rightarrow \nabla_p &= \frac{4U}{l_m}\xi^2 + \nabla_{\mathrm{ad}}\end{aligned} \tag{17}$$

The relation between the temperature gradients are

$$\nabla_{\mathrm{ad}} < \nabla_{\mathrm{p}} < \nabla^* < \nabla_{\mathrm{stable}} \tag{18}$$

C. Instability criterion

The instability criterion is defined as

$$\nabla > \nabla_{\mathrm{ad}} \tag{19}$$

and says if the temperature gradient for the star is lower than the adiabatic temperature gradient, then we have convective instability [1]. In this case, the gas/parcel will begin to move and we use the eq. 4 for $\partial T/\partial m$. If we do not have convective instability, then eq. 5 is used for $\partial T/\partial m$. This criterion must be checked at each mass shell of our stellar model.

D. Pressure

In a star, there are several forces that may contribute to the pressure. In the case of our Sun, it is mainly gas pressure and radiative pressure to a small degree. The radiative pressure depends only on temperature and not density

$$P_{\text{rad}} = \frac{a}{3}T^4 \tag{20}$$

where a is the radiation density constant defined as

$$a = \frac{4\sigma}{c} \tag{21}$$

where c is the speed of light. Gas pressure can be expressed through the equation of state for an ideal gas

$$P_{\text{gas}} = \frac{\overbrace{N}^{m/(\mu m_u)}}{V} k_B T = \underbrace{\frac{m}{V}}_{\rho} \frac{k_B T}{\mu m_u} = \frac{\rho k_B T}{\mu m_u} \tag{22}$$

where V is volume, and N is the number of particles. Thus, giving us the total pressure in a star to be

$$P = P_{\text{gas}} + P_{\text{rad}} = \frac{\rho k_B T}{\mu m_u} + \frac{a}{3}T^4 \tag{23}$$

We see that gas pressure in a star is related to the microphysics through the average weight of the particles μ. The mean molecular weight per particle is calculated with the following expression

$$\mu = \frac{1}{\left(\sum \frac{\text{free particles per ion}}{\text{nucleons per ion}} \cdot \text{ion mass fraction}\right)} \tag{24}$$

From the pressure we obtain the following equation for density, ρ

$$\rho = \frac{P \mu m_u}{k_B T} \tag{25}$$

III. METHOD

A. Mean molecular weight

The mean molecular weight μ is calculated through eq 24. We consider the fully ionized case for all elements. Thus, "ion mass fraction" is 1 for all elements, and "free particles" become the number of atoms (= 1 per element) plus the number of free electrons.

$$\mu = \frac{1}{2X + \mathrm{Y}_2^3\mathrm{He} + \frac{3}{4}Y + \frac{4}{7}\mathrm{Z}_3^7\mathrm{Li} + \frac{5}{7}\mathrm{Z}_4^7\mathrm{Be} + \frac{8}{14}\mathrm{Z}_7^{14}\mathrm{N}} \tag{26}$$

Table II: Mass fraction of elements in our model

Symbol	Element	Value
X	Hydrogen	0.7
$\mathrm{Y}_2^3\mathrm{He}$	Helium-3	10^{10}
Y	Helium-4	0.29
$\mathrm{Z}_3^7\mathrm{Li}$	Lithium-7	10^{-7}
$\mathrm{Z}_4^7\mathrm{Be}$	Beryllium-7	10^{-7}
$\mathrm{Z}_7^{14}\mathrm{N}$	Nitrogen-14	10^{-11}

B. Opacity

Opacity, κ, is obtained from `opacity.txt`. The structure of the .txt file is as follows:

- The top row is $\log_{10}(\mathrm{R})$, where $R \equiv \frac{\rho}{(T/10^6)^3}$ and ρ is given in cgs units [g/cm^3].
- The first column is $\log_{10}(\mathrm{T})$, with T given in K.
- The rest of the table is $\log_{10}(\kappa)$ given in cgs units [cm^2/g].

In the program, there is a function that takes T and ρ as inputs and returns κ. The table is interpolated for the case where the input values are not exactly found using `scipy.interpolate.RectBivariateSpline`. In the case where input values are not found in the table, the method extrapolates, and the program outputs a warning.

C. Integration

The four partial differential equations are numerically solved using Euler's method with variable step length [2].

$$\begin{aligned} dV &= f\ dm \\ V_{i+1} &= V_i + dV \end{aligned} \tag{27}$$

V is the variable we are interested in calculating for each iteration, f is the absolute value of the PDEs (in our case: equations 1, 2, 3 and 4). dm is a variable step length defined as

$$dm = \text{MIN}\left[\frac{pV}{f}\right] \tag{28}$$

where p is a fraction that V is allowed to change, 0.1 is a safe place to start. Since there are four governing equations, there will be produced dm for them all, but the smallest is chosen. We are interested in creating a stellar model which solves V from the surface and to the core. This indicated that either dm needs to be negative or dV in eq. 27 to be negative.

D. Convective instability

A check for convective instability (eq. 19) is included at each mass shell by an if-statement. This determines what expression for $\partial T/\partial m$ to use. It also determines the temperature gradient of the star, and whether there is convective flux or not. If the instability criterion is fulfilled, there is convective flux and ∇^* is equal to eq. 13. Otherwise, $F_{\text{con}} = 0$ and $\nabla^* = \nabla_{\text{stable}}$.

E. Best model

To achieve the goals of this model, the initial values must be modified. Before doing so, we change each of them individually to see how the different parameters impact the model. We investigate the following values: R_0, T_0, ρ_0, and P_0.

IV. RESULTS

The mean molecular weight of our model, defined in eq. 26, is approximately 0.618.
From investigating how the different parameters individually impact the stellar model, these are our keynotes:

- Increase of T_0 helps to achieve luminosity being within 5% of given initial condition L_0.
- Increase of ρ_0 by at least a factor of 30, gives a continuous convection zone near the surface with a width of at least 15% of R_0. However, the luminosity also increases.
- Increasing P_0 would widen the convection zone near the surface, but also the convection zone inside the core. In most cases, the convection zone inside the core would be wider than the one near the surface.
- Small changes in the initial radius make a big impact on the model, and we discovered that a change of factor 1.5 or larger causes an overflow in the program.

More detailed results from this investigation, including figures can be found in appendix B. With these keynotes in mind, we had an idea of what combinations of parameters we could change to achieve our goals. The parameters we ended up changing are found in table III

Table III: Inital parameters used to achieve the goals of our model.

Mass	Radius	Luminosity	Density	Temperature
$M_\odot$	$0.9R_\odot$	$1.2L_\odot$	$29\bar{\rho}_\odot$	2885 K

Our final model has a mass going to 0, radius to 4.3% of R_0, and luminosity to 4.1% of L_0. The core is reaching out to approximately 26.9% of R_0, and there is a continuous convection zone present near the surface of the star with a width of around 16.2% of R_0. A small convection zone can be found near the center but it is smaller than the "main" convection zone near the surface. A cross-section of our final model is presented in figure 1.

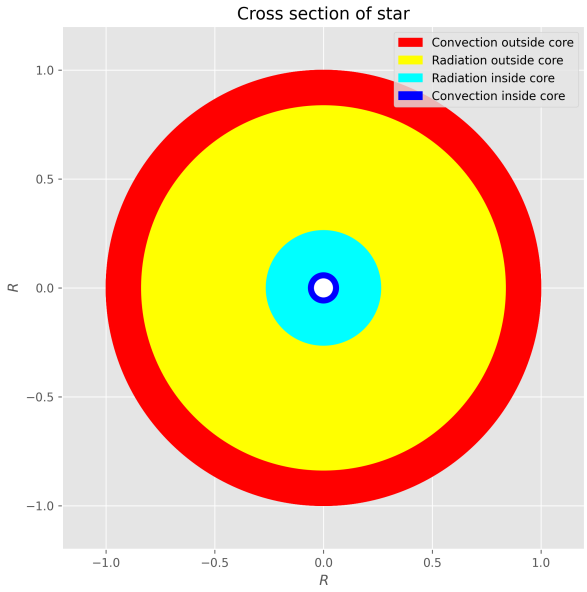

Figure 1: Cross section of our final model which fulfills our goals.

Figure 2 shows the evolution of the following parameters: M/M_0, L/L_0, T, R/R_0, and ρ/ρ_0, as a function of radius.

Figure 3 shows relative flux or relative energy being transported by convection and radiation (F_{con} and F_{rad}) as functions of radius.

In figure 4 we find ∇_{stable}, ∇_{ad}, and ∇^* as a function of radius with a logarithmic y-axis.

Figure 5 shows the relative energy production from the PP chains and CNO cycle as a function of radius. $\varepsilon/\varepsilon_{max}$ is included in order to estimate how much each branch contributes to the overall luminosity at a given radius. ε_{max} is the sum of energy produced by the PP chains and CNO cycle.

V. DISCUSSION

Key points presented at the beginning of section IV are from running a couple of experiments with changing

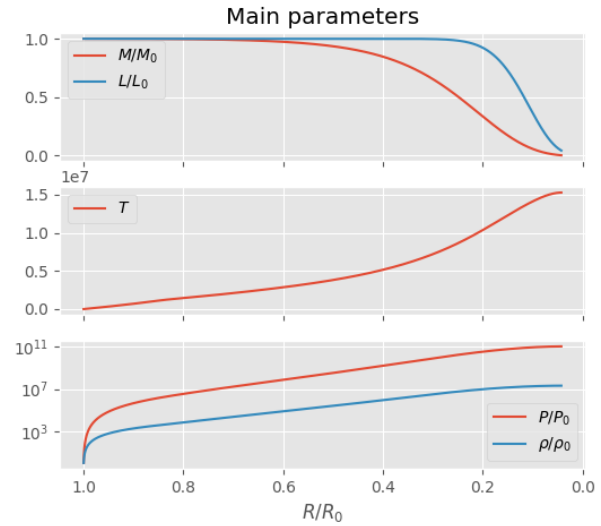

Figure 2: Evolution of main parameters from the surface of the star to the core.

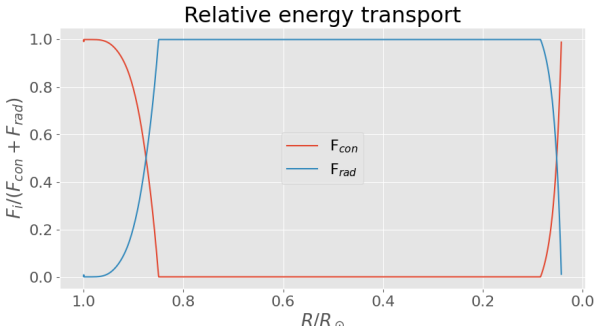

Figure 3: Fraction of energy being transported by convection and radiation as a function of radius.

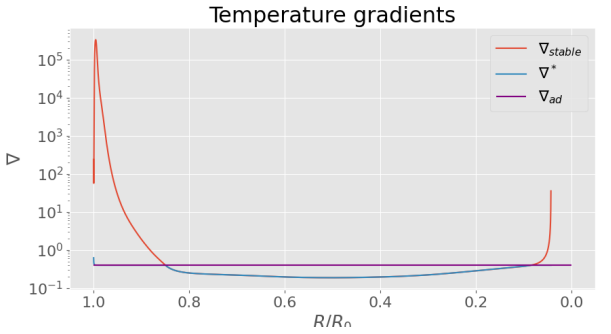

Figure 4: Temperature gradients for our final model with a logarithmic scale on the y-axis.

several parameters individually to see how they impact the model. From this, we see that changing the initial parameters for ρ_0 will give us a wider convection zone near the surface. Another possibility is to change P_0

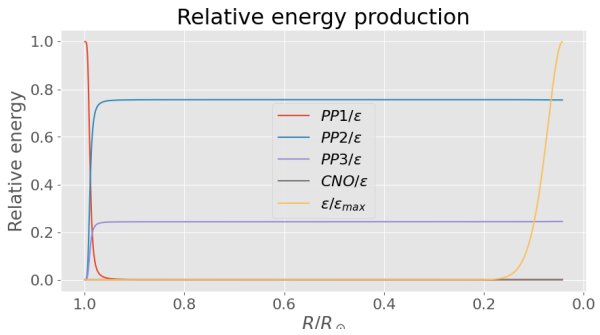

Figure 5: Relative energy production from PPI, PPII, PPIII, and CNO as a function of radius, as well as $\varepsilon/\varepsilon_{\max}$.

but at risk of creating a convection zone in the core of the same width. A difficulty that arose was finding the balance between parameters that could fulfill the goals for luminosity and convection. In various cases, the parameters which gave a model satisfying the width of the convection zone would give $L/L_0 \sim 50\%$. Otherwise, luminosity would go to at least within 5% of L_0, but the convection zone be too thin.

When changing all the variables simultaneously, I noticed there was in fact not a sufficient amount of experimenting done. Due to this, I was unaware of the parameter's limits which led to overflows in my program numerous times. Most of the parameters were also tweaked by similar factors during the investigation, thus giving a small range of variety in results. This made it difficult to predict what would happen outside of the factors tested. Finding the best model would have been more straightforward, had I increased the number of experiments and variety in factors multiplied with the initial values.

By changing the initial value of T_0, the results for luminosity remained somewhat similar. This is due to how luminosity is calculated in Project 1. Temperature appears when computing the proportionality function λ_{ik}, but scaled where $T_9 = T \cdot 10^{-9}$. Thus, temperature contributes to luminosity only by a small degree. T_0 and R_0 barely affect convection and radiation. By looking at the expression for total flux in eq. 6 with ∇_{stable} inserted, we see the contribution from T cancel each other. The remaining contribution is from R, but due to the division of a large number, the result is a small number.

The main parameters are visualized in figure 2. In the upper plotting window, we can easily see how M/M_0 and L/L_0 approach 5% of their initial value as we move towards the core. This was expected as it was one of the goals driving this stellar modeling. In the second and third plotting windows, we see the evolution of T, P/P_0, and ρ/ρ_0. All three parameters increase drastically as we reach the core. To get an intuition of how reasonable these values may be, we can compare them with our

Sun. The solar parameters of the core are fetched from Appendix B in ref. [1], and the values of our model are read from figure 2. Table IV shows us how the value of

Table IV: Comparison of solar parameters and our model's parameters.

	Temperature [K]	**Density** [kg m^{-3}]	**Pressure** [Pa]
The Sun	$1.57 \cdot 10^7$	$1.62 \cdot 10^5$	$3.45 \cdot 10^{16}$
Our model	$1.5 \cdot 10^7$	10^7	10^{11}

our star and the Sun is somewhat within the same order of magnitude, thus our parameters are reasonable.

Our final cross-section is visualized in fig. 1. The width of its core and convection zone near the surface was determined by a brute force method. Rather than having my program compute the width of these layers, I manually checked it in my plot. Nevertheless, we compare our star to the Sun. The convection zone of the Sun is approximately 28.7% of $R_\odot$ in width ($\simeq 2 \cdot 10^8$ m) [3], and its core reaches out to $0.2R_\odot$ ($\simeq 1.392 \cdot 10^8$ m) [4]. Our star has a convection zone at the surface with a width of approximately 16.2% ($\simeq 1.01 \cdot 10^8$ m) of R_0 and a core reaching out to 26.9% of R_0 ($\simeq 1.68 \cdot 10^8$ m). Based on these numbers, we see that our star has a smaller convection zone than the Sun, but a larger core. However, they both have the same mass and somewhat similar radius.

Relative energy production as a function of radius is shown in figure 5. In Project 1 we plotted the relative energy production from each of the PP branches and the CNO cycle as a function of temperature in the interval $T \in [10^4, 10^9]$. Both figures look to be almost identical. However, it is hard to tell if PP1 stops dominating faster in this project, or if the axis has a tighter layout. It would be more helpful to add a secondary axis figure 5 for temperature. Our model has a temperature interval $T \in [10^3, 10^7]$ (as discussed when looking at the evolution of temperature). If we cut the plot from Project 1 at 10^7 K, we see both plots are identical in shape. The difference is a lack of contribution from the CNO cycle in our model. In Project 1 we found that the CNO cycle dominates for temperatures above 10^8 K and since our core does not reach such magnitude, we expect no contribution from the CNO cycle. $\varepsilon/\varepsilon_{max}$ (yellow graph) was added in order to estimate how much each branch contributes to the overall luminosity at a given radius. The contribution to the luminosity comes from the stellar core, as we see the yellow graph is present from around where the core of our model begins. In that region, we see the contribution comes mainly from PP2 (slightly below 80%) and a little from PP3 (slightly above 20%). PP1 and CNO cycle does not contribute to the overall luminosity of our star.

Figure 3 shows the fraction of energy being transported by convection and radiation both as functions of radius. We expect correspondence with the layer widths of the cross-section in the figure. By looking at figure 1, we expect energy to be transported by convection at the surface, followed by radiation throughout most of the star, and finally convection by the end. This is the exact case in figure 3. We start out with convective flux, followed by radiative flux, and lastly, convection once again. We see the convective flux in the core is carried throughout a smaller section of the Sun, than the convective flux near the surface. This corresponds well to the different widths of the convection zones shown in the cross-section.

Figure 4 shows the temperature gradients in our star. We already know from looking at the cross-section (fig. 1) and relative energy transport (fig. 5), that we have convection near the surface and in the core. Thus, indicating the instability criterion is fulfilled in said regions. In the plot, we see that the graph for ∇_{stable} is present near the surface and in the core. Additionally, ∇_{stable} dominates for a larger region near the surface, than in the core. This corresponds well with our cross-section.

VI. CONCLUSION

The purpose of this paper was to create a Sun-like model which fulfilled the goals listed in the introduction. This was fulfilled by changing $R_\odot \to 0.9R_\odot$, $L_\odot \to 1.2L_\odot$, $\bar{\rho}_\odot \to 29\bar{\rho}_\odot$, and $T_\odot \to 0.5R_\odot$ ($M_\odot$ was kept the same). The result was a cross-section with a convection zone near the surface with a width of approximately 16.2% of R_0, and a core reaching out to 26.9% of R_0. Our cross-section has a larger core and a more narrow convection zone near the surface, compared to the Sun. The mass goes to 0, while the radius goes to 4.3% of R_0 and luminosity to 4.1% of L_0. The relative energy of production of our model vs. Project 1 shows similarities. The difference is the lack of contribution from the CNO cycle as our core does not reach a high enough temperature for that to happen. The plot also shows that PP2 and PP3 are the ones contributing to the overall luminosity of our star.

Although this model fulfills the goals set for this project, it is not unique. If time allowed, I would have experimented with parameters that gave a different model. Perhaps a model where the CNO cycle contributed to the energy production of the star.

Appendix A: Derivation of useful expression

1. Pressure scale height

Assume a static atmosphere with two forces present: pressure and gravity. Gravity is assumed to be represented by a constant gravitational acceleration g and aligned along $-r$. The Navier-Stokes equations

$$\frac{\partial}{\partial t}(\rho \cdot \vec{u}) + \frac{\partial}{\partial t}(\rho \vec{u} \otimes \vec{u}) = -\vec{\nabla} P + \cancelto{0}{\vec{\nabla} \tau} + \rho \vec{g} \tag{A1}$$

describes the unit volume of gas or liquid. The left-hand side describes the momentum of the fluid and the right-hand side gives a description of everything that accelerates. Since we assume a static atmosphere, the Navier-stokes equation reduces to

$$0 = -\underbrace{\vec{\nabla} P}_{\partial P / \partial r} + \rho \vec{g} \tag{A2}$$

In this task, we also assume an ideal gas. Thus the expression for density ρ is

$$\rho = \frac{P m_u \mu}{k_B T} \tag{A3}$$

Inserting eq. A3 into eq. A2 gives

$$\frac{\partial P}{\partial r} = P \frac{\mu m_u}{k_B T} \vec{g} \tag{A4}$$

The expression for pressure scale height is

$$H_P = -P \frac{\partial r}{\partial P} \tag{A5}$$

By inserting eq. A4 into the expression for pressure scale height we obtain

$$H_P = -\cancel{P} \cdot \left(-\frac{k_B T}{\mu m_u \cancel{P} \vec{g}} \right) = \frac{k_B T}{\mu m_u \vec{g}} \tag{A6}$$

The reason for negative $\partial r / \partial P$ is because for our model we will be integrating from the surface of the star to the core.

2. Geometric factor

The geometric factor is defined as $S/(Qd)$ where S is the surface area, d is diameter, and Q is the surface normal to velocity v. For a spherical parcel with radius r_p, the geometric factor becomes

$$\frac{S}{Qd} = \frac{4\pi r_p^2}{2 r_p \cdot \pi r_p^2} = \frac{2}{r_p} \tag{A7}$$

and $r_p = l_m/2$ where l_m is mixing length.

3. Expression for $(\nabla^* - \nabla_p)$

We wish to obtain an expression for $(\nabla^* - \nabla_p)$ as a function of ∇^* and ∇_{stable} by inserting equation 5.80 and 5.82 into 5.81 from AST3310 lecture notes.
Equation 5.80 from lecture notes is

$$F_{\text{con}} = \rho c_p T \sqrt{g \delta} H_P^{-3/2} \left(\frac{l_m}{2} \right)^2 (\nabla^* - \nabla_p)^{3/2} \tag{A8}$$

Equation 5.82 is

$$F_{\text{rad}} = \frac{16\sigma T^4}{3\kappa\rho H_P}\nabla^* \tag{A9}$$

Last we have equation 5.81 (hereby: eq. A10), in which 5.80 (hereby: eq. A8) and 5.82 (hereby: eq. A9) will be inserted into

$$F_{\text{rad}} + F_{\text{con}} = \frac{16\sigma T^4}{3\kappa\rho H_P}\nabla_{\text{stable}} \tag{A10}$$

Inserting eq. A8 and eq. A10 in . A10 we obtain

$$\begin{aligned}
\rho c_p T\sqrt{g\delta}H_P^{-3/2}\left(\frac{l_m}{2}\right)^2(\nabla^*-\nabla_p)^{3/2} + \frac{16\sigma T^4}{3\kappa\rho H_P}\nabla^* &= \frac{16\sigma T^4}{3\kappa\rho H_P}\nabla_{\text{stable}} \\
\rho c_p T\sqrt{g\delta}H_P^{-\cancel{3}^{1}/2}\left(\frac{l_m}{2}\right)^2(\nabla^*-\nabla_p)^{3/2} &= \frac{16\sigma T^4}{3\kappa\rho\cancel{H_P}}(\nabla_{\text{stable}-\nabla^*}) \\
(\nabla^*-\nabla_p)^{3/2} &= \underbrace{\frac{64\sigma\cancel{T^4}^{3}}{3\kappa\rho^2 c_p\cancel{T}}\sqrt{\frac{H_P}{g\delta}}}_{U} l_m^{-2}(\nabla_{\text{stable}-\nabla^*}) \\
(\nabla^*-\nabla_p)^{3/2} &= l_m^{-2}U(\nabla_{\text{stable}}-\nabla^*)
\end{aligned} \tag{A11}$$

where

$$U = \frac{64\sigma T^3}{3\kappa\rho^2 c_P}\sqrt{\frac{H_P}{g\delta}} \tag{A12}$$

4. Second order equation for $(\nabla^*-\nabla_p)^{1/2}\equiv\xi$

To get a second order equation for $(\nabla^*-\nabla_p)^{1/2}$, we insert equation 5.74 from lecture notes [1] into

$$(\nabla_p-\nabla_{\text{ad}}) = (\nabla^*-\nabla_{\text{ad}}) - (\nabla^*-\nabla_p) \tag{A13}$$

where eq. 5.74 (hereby, eq. A14) is

$$(\nabla_p-\nabla_{\text{ad}}) = \frac{32\sigma T^3}{3\kappa\rho^2 c_p v}\frac{S}{Qd}(\nabla^*-\nabla_p) \tag{A14}$$

From equation 5.70 in lecture notes (hereby, eq. A15) we obtain the expression for v

$$v = \sqrt{\frac{g\delta}{H_P}}\frac{l_m}{2}\underbrace{(\nabla^*-\nabla_p)^{1/2}}_{\xi} = \sqrt{\frac{g\delta}{H_P}}\frac{l_m}{2}\xi \tag{A15}$$

where $\xi = (\nabla^*-\nabla_p)^{1/2}$.
By inserting eq. A14 into eq. A13 we get the following

$$\begin{aligned}
\frac{32\sigma T^3}{3\kappa\rho^2 c_p\underbrace{v}_{eq.A15}}\frac{S}{Qd}\underbrace{(\nabla^*-\nabla_p)}_{\xi^2} &= (\nabla^*-\nabla_{\text{ad}}) - \underbrace{(\nabla^*-\nabla_p)}_{\xi^2} \\
\underbrace{\frac{64\sigma T^3}{3\kappa\rho^2 c_p\sqrt{\frac{g\delta}{H_P}}\cancel{\xi}}}_{U}\frac{S}{Qdl_m}\xi^{\cancel{2}^{1}} &= (\nabla^*-\nabla_{\text{ad}}) - \xi^2 \\
\xi^2 + U\underbrace{\frac{S}{Qdl_m}}_{k}\xi - (\nabla^*-\nabla_{\text{ad}}) &= 0 \\
\xi^2 + Uk\xi - (\nabla^*-\nabla_{\text{ad}}) &= 0
\end{aligned} \tag{A16}$$

Roots of ξ are

$$\Rightarrow \xi = \frac{-k \pm \sqrt{k^2 + 4(\nabla^* - \nabla_{\rm ad})}}{2} \tag{A17}$$

To find the viable solution(s) we need to look at the definition of ξ. For the gas parcel to rise, ∇_p must be smaller than ∇^*, i.e. $\nabla_p < \nabla^* \Rightarrow \xi = (\nabla^* - \nabla_p)^{1/2} > 0$. The only viable solution for ξ is

$$\xi = \frac{-k + \sqrt{k^2 + 4(\nabla^* - \nabla_{\rm ad})}}{2} \tag{A18}$$

5. Cubic polynomial for solving for ξ

To eliminate ∇^* in eq. A11, we use our results from eq. A16.
We begin by expressing eq. A16 in terms of ∇^*

$$\begin{aligned} \xi^2 + k\xi - (\nabla^* - \nabla_{\rm ad}) &= 0 \\ \nabla^* &= \xi^2 + k\xi + \nabla_{\rm ad} \end{aligned} \tag{A19}$$

followed by rewriting eq. A11 and insert eq. A19

$$\begin{aligned} \underbrace{(\nabla^* - \nabla_p)^{3/2}}_{\xi^3} &= l_m^{-2} U (\nabla_{\rm stable} - \nabla^*) \\ \xi^3 &= l_m^{-2} U (\nabla_{\rm stable} - \underbrace{\nabla^*}_{eq.A19}) \\ \xi^3 &= l_m^{-2} U (\nabla_{\rm stable} - \xi^2 - k\xi - \nabla_{\rm ad}) \end{aligned} \tag{A20}$$

$$\xi^3 + l_m^{-2} U \xi^2 + l_m^{-2} U k \xi - l_m^{-2} U (\nabla_{\rm stable} - \nabla_{\rm ad}) = 0 \tag{A21}$$

This cubic polynomial will have three roots where two of which are complex and the third one is real. However, since $\xi > 0$, only the real root is a viable solution.

Appendix B: Investigation

Table V: Results from investigating the change of parameters. ”-” indicates that the initial value was kept the same.

R_0	T_0	P_0	ρ_0	M/M_0	R/R_0	L/L_0	Figure
-	$2T_0$	-	-	0%	7%	9%	6
-	$4T_0$	-	-	0%	7%	8.8%	7
-	$0.2T_0$	-	-	0%	6.9%	10.3%	8
-	-	-	$10\rho_0$	0%	6.4%	26.6%	9
-	-	-	$50\rho_0$	0%	4.2%	51.1%	10
-	-	-	$30\rho_0$	0%	5.4%	42.6%	11
-	-	$5P_0$	-	0%	6.7%	18.7%	12
-	-	$40P_0$	-	0%	4.8%%	47.3%	13
-	-	$20P_0$	-	0%	5.9%	36.3%	14
$1.1R_0$	-	-	-	0%	5.5%	34%	15
$1.2R_0$	-	-	-	0%	3.7%	49.6%	16
$1.25R_0$	-	-	-	0%	2.3%	55.0%	17

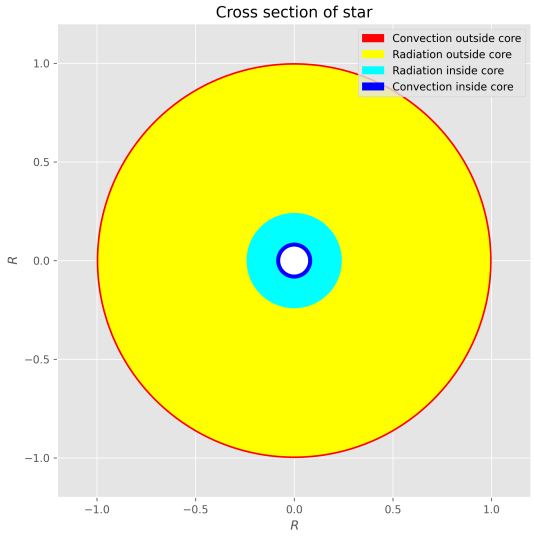

Figure 6: Parameter change of $T0 \rightarrow 2T_0$

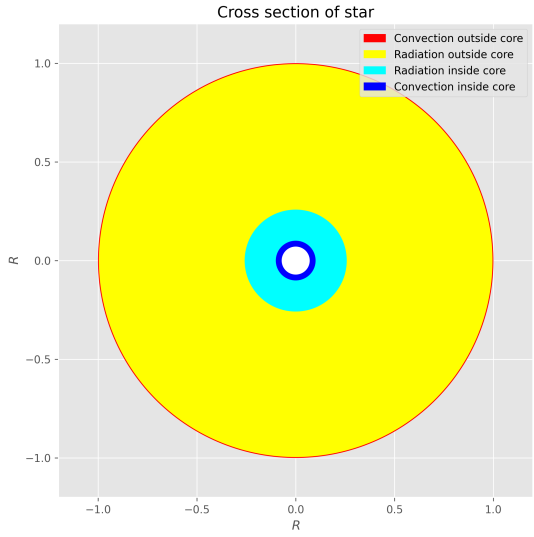

Figure 7: Parameter change of $T0 \rightarrow 4T_0$

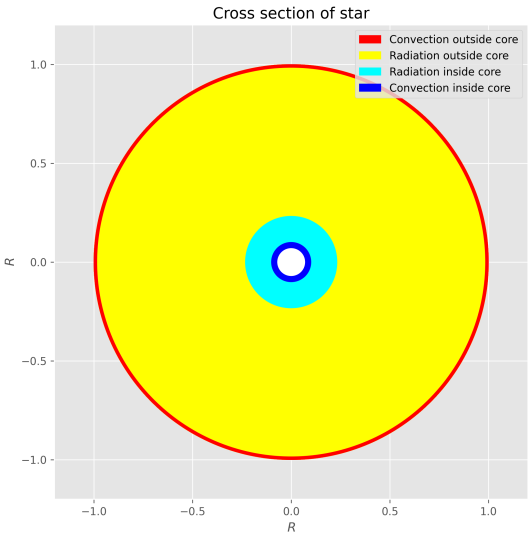

Figure 8: Parameter change of $T0 \rightarrow 0.2T_0$

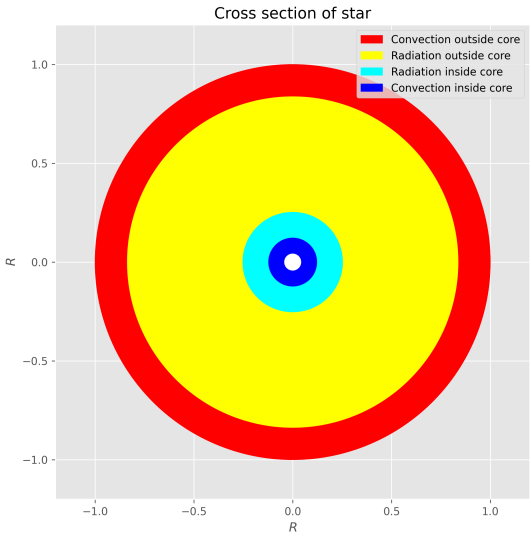

Figure 10: Parameter change of $\rho_0 \rightarrow 50\rho_0$

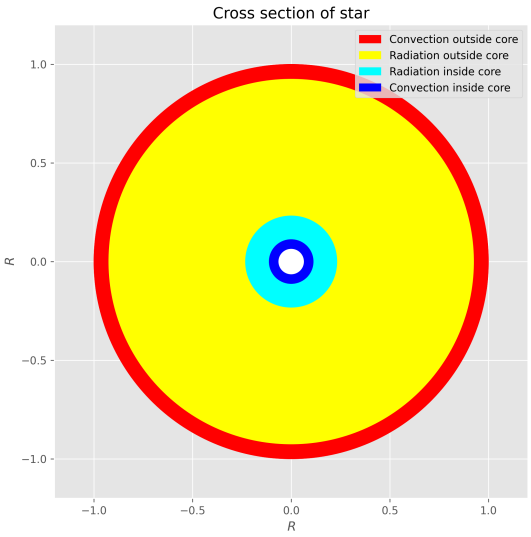

Figure 9: Parameter change of $\rho_0 \rightarrow 10\rho_0$

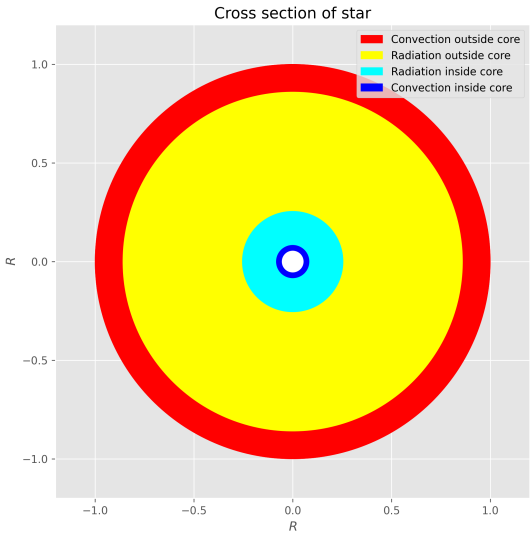

Figure 11: Parameter change of $\rho_0 \rightarrow 30\rho_0$

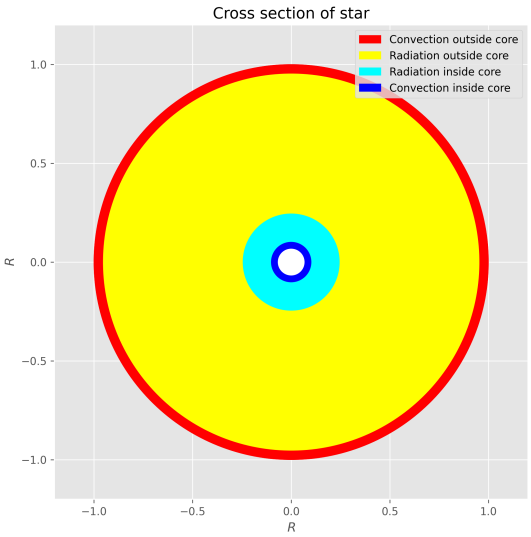

Figure 12: Parameter change of $P_0 \to 5P_0$

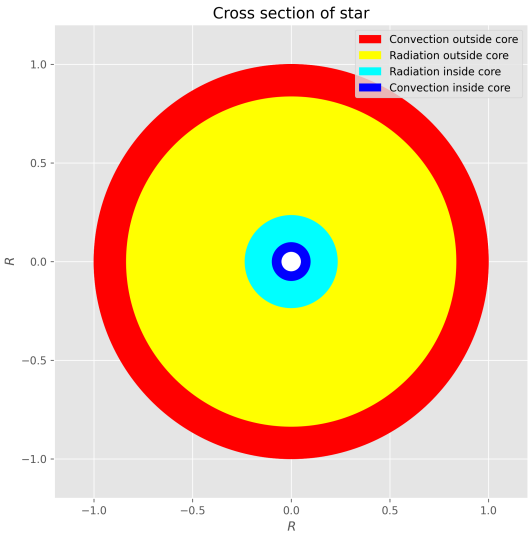

Figure 13: Parameter change of $P_0 \to 40P_0$

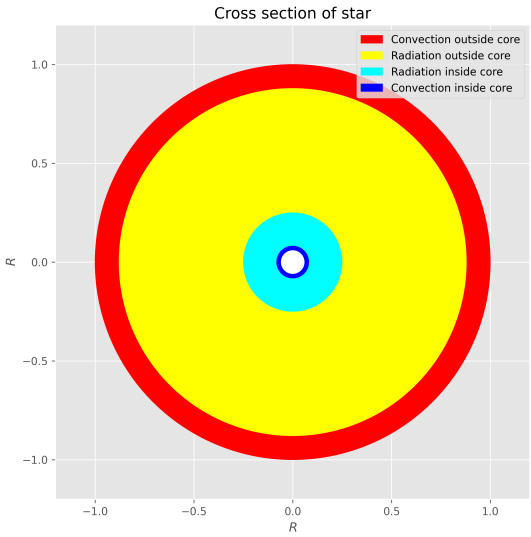

Figure 14: Parameter change of $P_0 \to 20P_0$

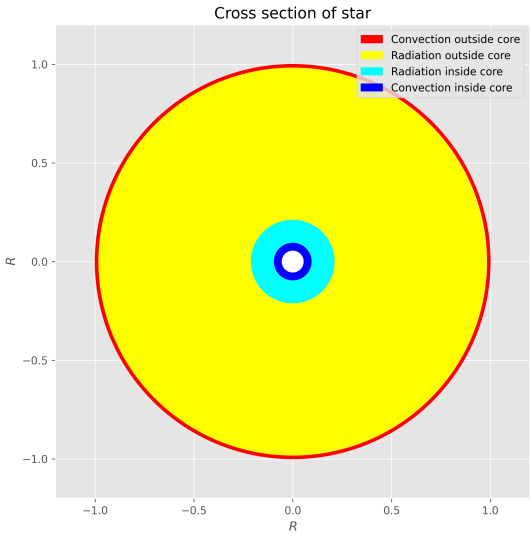

Figure 15: Parameter change of $R_0 \to 1.1R_0$

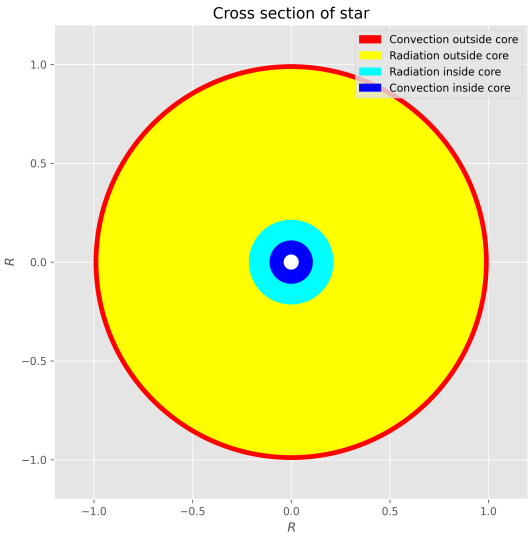

Figure 16: Parameter change of $R_0 \rightarrow 1.2R_0$

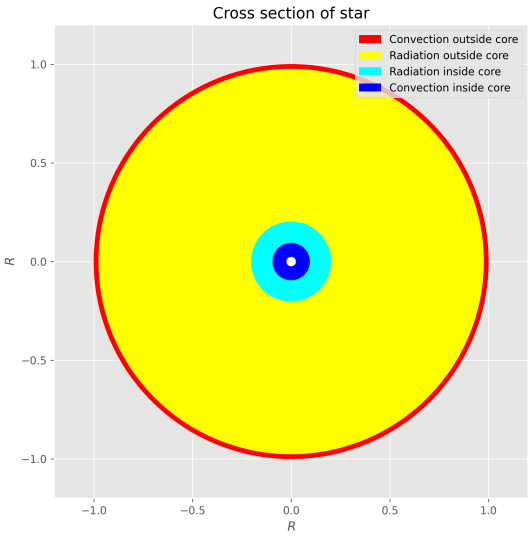

Figure 17: Parameter change of $R_0 \rightarrow 1.25R_0$

Appendix C: Sanity checks

Table VI: A check to see if the interpolation of opacity values gives reasonable outputs.

$\log_{10}T$	$\log_{10}R$ (cgs)	$\log_{10}\kappa$ (cgs) (expected)	κ (SI) (computed)	$\log_{10}\kappa$ (cgs) (expected)	κ (SI) (computed)
3.750	-6.00	-1.55	-1.546000	0.00284	0.002844
3.755	- 5.95	-1.51	-1.502573	0.00311	0.003144
3.755	- 5.80	-1.57	-1.567107	0.00268	0.002710
3.755	- 5.70	-1.61	-1.609850	0.00246	0.002456
3.755	- 5.55	-1.67	-1.673324	0.00212	0.002122
3.770	- 5.95	-1.33	-1.312074	0.00470	0.004874
3.780	- 5.95	-1.20	-1.190270	0.00625	0.006453
3.795	- 5.95	-1.02	-1.018097	0.00945	0.009592
3.770	- 5.80	-1.39	-1.374133	0.00405	0.004225
3.775	- 5.75	-1.35	-1.331313	0.00443	0.004663
3.780	- 5.70	-1.31	-1.288318	0.00494	0.005149
3.795	- 5.55	-1.16	-1.157945	0.00689	0.006951
3.800	- 5.50	-1.11	-1.114000	0.00769	0.007691

Table VII: Sanity check from example 5.1 in ref. [1]

	$\nabla_{\rm stable}$	$\nabla_{\rm ad}$	∇^*	H_P	U	ξ	v	$\frac{F_{\rm con}}{F_{\rm con}+F_{\rm rad}}$	$\frac{F_{\rm rad}}{F_{\rm con}+F_{\rm rad}}$
Expected	3.26	0.4	0.4	32.4	594000	0.001173	65.6	0.88	0.12
Computed	3.16053	0.4	0.400001	31.4	603441	0.001189	65.407	0.873438	0.126562

Further check to see if eq. 5.83 holds:

```
nabla_stable > nabla* > nabla_p > nabla_ad satisfied?: True
```

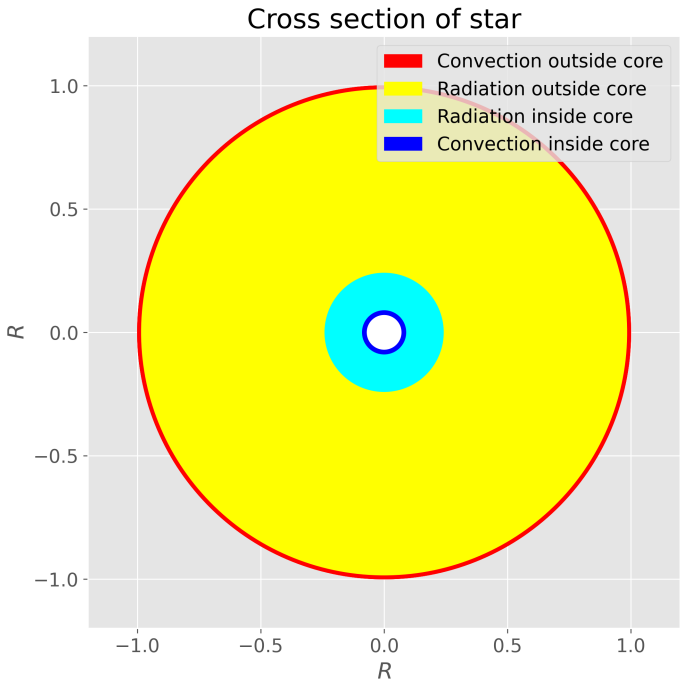

Figure 18: Model verification: Cross section of our star given initial conditions.

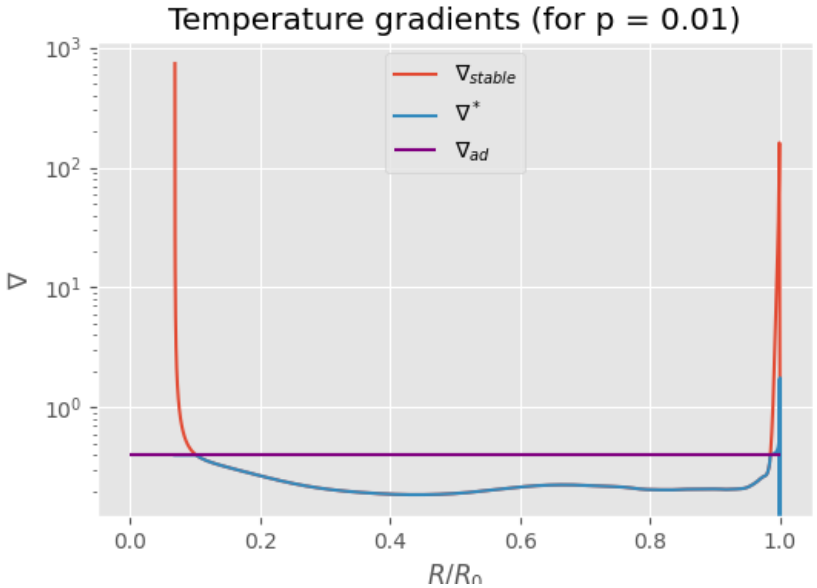

Figure 19: Model verification: Temperature gradient plot given initial conditions.

Appendix D: References

[1] Gudiksen, B. AST3310: Astrophysical plasma and stellar interiors. [PDF].
[2] Gudiksen, B. VARIABLE STEPLENGTH. [PDF]
[3] (n.d.). The Solar Interior. NASA. [Website]
[4] (2007). Tracking Solar Gravity Modes: The Dynamics of the Solar Core. SCIENCE, 316(5831). https://doi.org/10.1126/science.1140598